PHYSICAL REVIEW B **71**, 180406(R) (2005)

Schottky barrier and spin polarization at the Fe_3O_4-Nb:$SrTiO_3$ interface

M. Ziese,* U. Köhler,† A. Bollero, R. Höhne, and P. Esquinazi
Division of Superconductivity and Magnetism, University of Leipzig, 04103 Leipzig, Germany
(Received 7 January 2005; published 25 May 2005)

The interface between magnetite (Fe_3O_4) and Nb-doped $SrTiO_3$ shows typical characteristics of a Schottky barrier. The magnetoresistance was found to depend on the bias current through the junction. This can be understood within a model for a Schottky contact with a ferromagnetic component. The spin polarization of the magnetite layer was determined to be about 60%.

DOI: 10.1103/PhysRevB.71.180406 PACS number(s): 75.70.−i, 85.75.−d, 73.50.Jt

Spin electronics has attracted intense research activity in recent years. Studies have focused on all-metal devices, spin injection into conventional semiconductors and oxide spin electronics. The latter field appears promising due to the discovery of various magnetoresistance effects[1,2] as well as the potential to combine materials with different characteristics such as ferromagnets, ferroelectrics, and superconductors in a single device using heteroepitaxial growth techniques. Spin-polarized transport across a Schottky contact has been discussed as an efficient means for spin injection into semiconductors[3–5] and has been experimentally observed in junctions between conventional semiconductors and ferromagnets. In a related approach the formation of all-oxide *p-n* junctions has been investigated in a system formed from electron- and hole-doped manganites[6] as well as at the $La_{0.9}Ba_{0.1}MnO_3/Nb:SrTiO_3$ (Ref. 7) and $La_{0.29}Pr_{0.38}Ca_{0.33}MnO_3/AlN/Nb:SrTiO_3$ (Ref. 8) interface. In this paper the transport properties at the interface between magnetite (Fe_3O_4) and Nb-doped $SrTiO_3$ ($Nb:SrTiO_3$) are studied. The ferrimagnet magnetite is an attractive material, since it has a high Curie temperature of 860 K and an expected high spin polarization. Band-structure calculations have predicted a half-metallic state[9] and spin-resolved photoemission indeed indicates a spin polarization close to 100% at room temperature.[10] However, the situation is not as clear-cut as these studies suggest for the following reasons. Magnetite has a strongly correlated electron system and undergoes a simultaneous structural and electronic transition at the Verwey temperature.[11] At this transition the structure changes from a high-temperature cubic to a low-temperature monoclinic phase.[12] The nature of the electronic transition is often viewed as a charge-ordering transition of the Fe^{3+} and Fe^{3+} ions on the octahedral sites.[12] The Verwey temperature sensitively depends on oxygen content with values for stoichiometric bulk magnetite around 125 K. In magnetite a strong electron-phonon interaction leads to polaron formation and a narrowing of the electronic bands. Moreover, on-site Coulomb correlations[13] drive the charge-order transition and open a gap in the electronic spectrum below the Verwey transition. The presence of strong electronic correlations casts doubts on the validity of band-structure models. Moreover, angular momentum coupling effects have been argued to lead to a reduced spin polarization of $-2/3$.[14,15] Here one considers the removal of a single electron from the fully relaxed wave function of a Fe^{2+} ion. Since the total wave function $|2,2\rangle$ can be written as

$$|2,2\rangle = \sqrt{\frac{5}{6}}\left|\frac{5}{2};\frac{5}{2}\downarrow\right\rangle - \sqrt{\frac{1}{6}}\left|\frac{5}{2};\frac{3}{2}\uparrow\right\rangle, \tag{1}$$

it follows that the effective spin polarization for the *removal* of a single electron from a Fe^{2+} ion is $P=-\sqrt{5/6}^2+\sqrt{1/6}^2=-2/3$.[15] $|J;m_J m_s\rangle$ denotes the product state composed of the core state and the free electron, with J and m_J being the total and the z component of the angular momentum of the core electrons, and m_s being the z component of the angular momentum of the extracted electron (spin up or spin down). $|J,m_J\rangle$ denotes the total wave function of Fe^{2+}. Moreover, the spectroscopic spin polarization must not necessarily agree with the transport spin polarization, since the former involves only the density of states, whereas the latter also depends on scattering times and Fermi velocities.[16] The only experimental estimate of the spin polarization in magnetite using transport techniques[17] yielded a spin polarization of 60% in agreement with the angular momentum coupling model. In general measurements of the spin polarization in magnetite are difficult because of its insulating character at low temperatures. The objectives of this paper are the study of the transport properties at the interface between magnetite and an oxidic normal metal, especially across the Verwey temperature, and the measurement of the transport spin polarization in magnetite using an alternative technique based on Schottky barrier formation. Clear evidence of a Schottky barrier at the Fe_3O_4-$Nb:SrTiO_3$ interface is presented that might be exploited in the construction of an all-oxide spin transistor.

Magnetite films were fabricated by pulsed laser deposition from a stoichiometric polycrystalline target onto single crystal $SrTiO_3$ (001) and $Nb(0.1\%):SrTiO_3$ (001) substrates. Substrate temperature and oxygen partial pressure during deposition were 430 °C and 1×10^{-5} mbar, respectively. X-ray diffractometry showed epitaxial growth with no difference between films on $SrTiO_3$ and $Nb:SrTiO_3$. Resistivity and magnetization measurements were performed on five magnetite films on $Nb:SrTiO_3$ with thicknesses between 55 and 176 nm. Verwey temperatures were determined from both magnetization and resistivity with values between 110 and 120 K without any systematic thickness dependence. All samples showed the same qualitative behavior; the data presented in this paper were measured on a magnetite film with a thickness of 70 nm. Magnetotransport measurements were performed in a continuous flow cryostat equipped with a

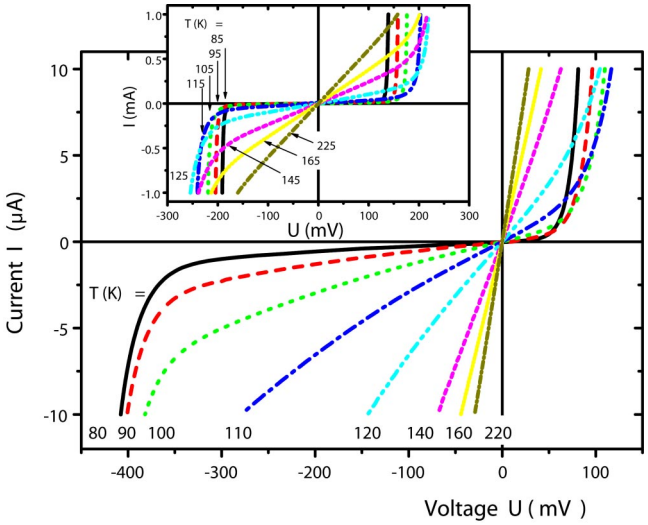

FIG. 1. (Color online) Current-voltage (*I-U*) curves of a Fe_3O_4-Nb:$SrTiO_3$ interface recorded in zero field at various temperatures as indicated. The inset shows the in-plane *I-U* characteristics at similar temperatures. Note the different current-axis scale.

9-T superconducting solenoid using a standard four-point technique. Measurements were performed on the as-grown films; lateral substrate dimensions were 5×5 mm^2. The samples were contacted using two indium contacts of sizes between 1×1 mm^2 and 2×5 mm^2 on the back of the substrate and silver paint or indium contacts of sizes between 1×1 and 2×5 mm^2 on the magnetite film. The form of the current-voltage characteristics was not observed to depend on contact area and material. Measurements were performed in in-plane and out-of-plane configurations, with mostly out-of-plane results presented here. The magnetic field was applied in plane and perpendicular to the current. The magnetite films on undoped $SrTiO_3$ were used as reference samples; these showed ohmic behavior of the in-plane resistivity in contrast to the films on the doped substrates. The Nb:$SrTiO_3$ substrates are metallic with a positive temperature coefficient of the resistivity and a carrier density of 5×10^{19} cm^{-3} as determined from Hall effect measurements. These substrates show a positive Lorentz-type magnetoresistance with a quadratic field dependence and magnetoresistance values at 3 T of 40%, 4%, and 0.4% at 20, 60, and 100 K, respectively.

Current-voltage (*I-U*) characteristics of the magnetite/Nb:$SrTiO_3$ interface recorded in zero applied field at various temperatures are shown in Fig. 1. In this current range the curves recorded at temperatures above 120 K are essentially linear, whereas a strong nonlinearity is seen below the Verwey transition. The *I-U* curves in the low-temperature regime are clearly asymmetric and characteristic for a Schottky barrier. The polarity is such that the forward bias corresponds to the application of a positive voltage to the substrate. The asymmetry of the *I-U* curves shows that Nb:$SrTiO_3$ acts as a metal and magnetite as a semiconductor in these junctions, which is consistent with the metallic conductivity of the substrate and the theoretical band structure of magnetite. For comparison *I-U* curves in the in-plane configuration are

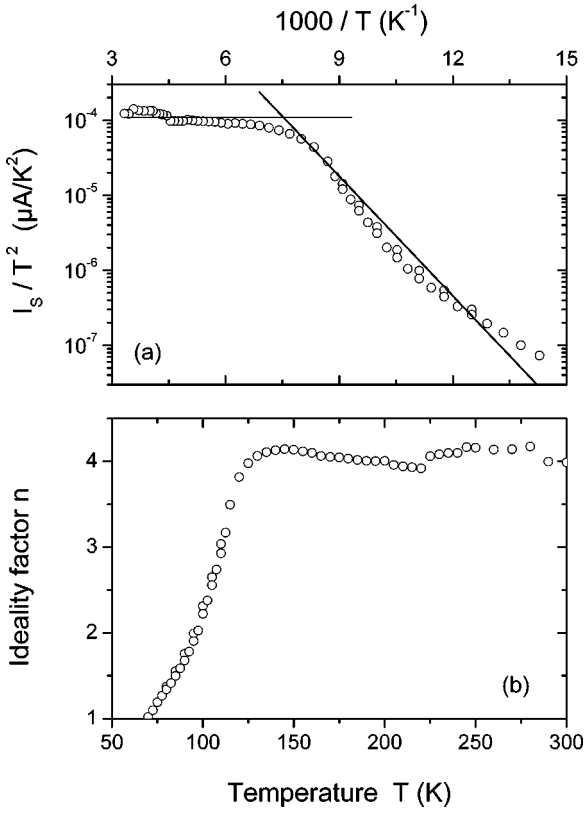

FIG. 2. (a) Reverse saturation current I_S divided by the square of the absolute temperature and (b) the ideality factor n of a Fe_3O_4-Nb:$SrTiO_3$ junction as a function of temperature.

shown in the inset to Fig. 1. These curves are also nonlinear, since the low-resistance substrate short circuits the high-resistance magnetite film for applied bias voltages sufficient to inject carriers across the interface barrier. In this configuration the *I-U* curves are symmetric, since there are always two junctions involved in carrier conduction. The out-of-plane data were analyzed within a thermionic emission model using

$$I = I_S\left[\exp\left(\frac{eU}{nk_BT}\right) - 1\right] + U/R, \tag{2}$$

with n, I_S, and R as parameters. The ohmic term is introduced to account for leakage currents and yields only a small contribution. From the data the ideality factor n and the reverse saturation current $I_S = SA^*T^2\exp(-e\Phi_B/kT)$ were extracted (see Fig. 2), where $A^* = em^*k_B^2/(2\pi^2\hbar^3)$ denotes the Richardson constant, e the electronic charge, m^* the effective mass, $\hbar$ Planck's constant, k_B the Boltzmann constant, Φ_B the Schottky barrier height, and S the junction area. The ideality factors ranged from 1 at low to 4 at high temperatures. This indicates that above the Verwey temperature the weak nonlinearity in the current-voltage curves might be due to some tunneling process, whereas a good, nearly ideal Schottky barrier is only formed below the Verwey temperature, when the gap in the electronic spectrum of magnetite has opened. The Schottky barrier height in zero field was determined from the reverse saturation current with

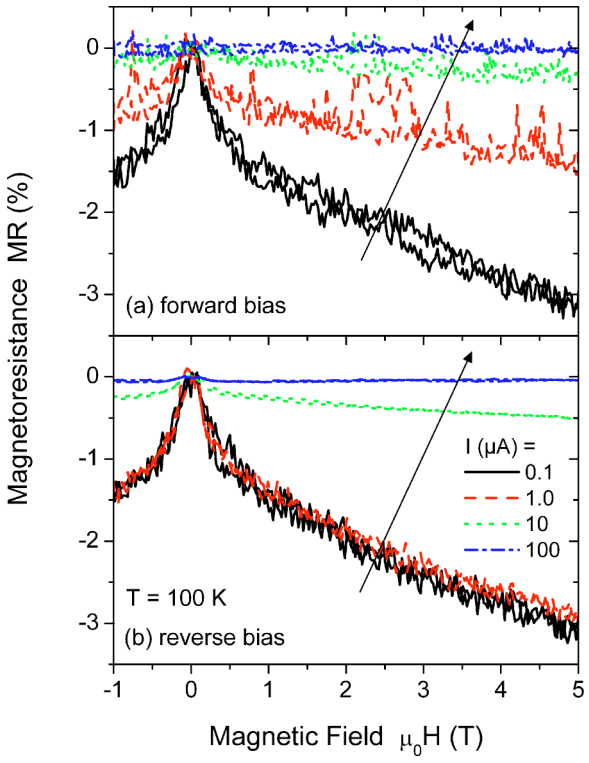

FIG. 3. (Color online) Magnetoresistance ratio $[U(B)-U(0)]/U(0)$ of a Fe_3O_4-Nb:$SrTiO_3$ junction measured at 100 K as a function of magnetic field at various current values for (a) forward and (b) reverse bias.

$\Phi_B=0.11\pm0.03$ eV below the Verwey transition and $\Phi_B=0\pm0.05$ eV above the transition. The uncertainty reflects both the fitting error and variations between the different samples. In essence, these data clearly show that a gap at the Fermi level opens in the electronic structure of magnetite below the Verwey transition.

Figure 3 shows the magnetoresistance ratio $[U(B)-U(0)]/U(0)$ measured at $T=100$ K and various currents as a function of the applied magnetic field. It is evident that the magnetoresistance has a strong bias dependence that proves that the magnetoresistance is an inherent property of the barrier and is not due to bulk scattering processes in the magnetite film. At high magnetic fields the magnetoresistance is linear in the applied field, whereas nonlinearities in the low field regime are due to domain reversal processes.

In the following we propose a model to account for the Schottky barrier magnetoresistance. Magnetite is a strongly correlated system with a gap in the electronic spectrum opening below the Verwey transition. In a first approximation this is modeled as a ferromagnetic semiconductor. The magnetoresistance at the barrier might arise from the Zeeman effect and will be derived in this paper in the two-current model.

Within thermionic emission theory the current density is given by[18]

$$j = A^* T^2 \exp\left(-\frac{e\Phi_B}{k_B T}\right)\left[\exp\left(\frac{eU}{nk_B T}\right)-1\right]. \tag{3}$$

The inset to Fig. 4 schematically shows the spin-split conduction bands assumed in this calculation with the definition

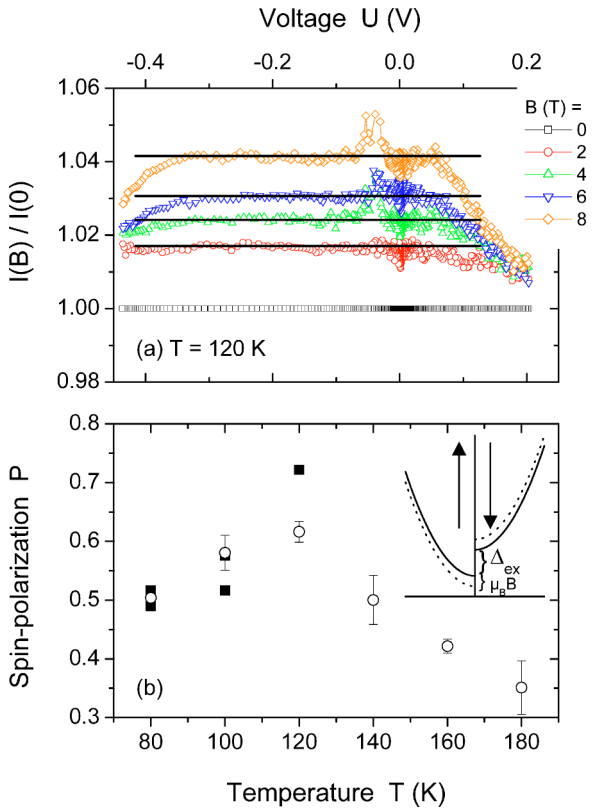

FIG. 4. (Color online) (a) Ratio of the current measured in an applied field B and in zero field as a function of the applied voltage bias. The straight lines are guides to the eye. (b) Spin polarization P determined from current-voltage curves (solid squares) and from magnetoresistance vs magnetic field curves (open circles). The inset to (b) shows the band structure assumed in the calculation with exchange splitting Δ_{ex} and Zeeman energy $\mu_B B$.

of the exchange energy Δ_{ex} and the Zeeman energy $\mu_B B$. The conduction band is assumed to be rigidly shifted by the exchange splitting Δ_{ex}. When a magnetic field is applied parallel to the spin polarization, the conduction-band edges are given by $E_{c\uparrow(\downarrow)}=E_c-(+)\Delta_{ex}/2-(+)\mu_B B$, where E_c is an average conduction-band edge. The g factor was assumed to be close to two and μ_B denotes the Bohr magneton. Accordingly, the potential barrier becomes spin and magnetic field dependent. In the two-current model the spin-dependent current densities are given by

$$j_{\uparrow(\downarrow)} = \frac{1}{2}A^* T^2 \exp\left(-\frac{e\Phi_B-(+)\Delta_{ex}/2-(+)\mu_B B}{k_B T}\right) \times\left[\exp\left(\frac{eU}{nk_B T}\right)-1\right]. \tag{4}$$

The total current density is then given by

$$j = (j_\uparrow + j_\downarrow) = A^* T^2 \exp\left(-\frac{e\Phi_B}{k_B T}\right)\cosh\left(\frac{\Delta_{ex}+2\mu_B B}{2k_B T}\right) \times\left[\exp\left(\frac{eU}{nk_B T}\right)-1\right]. \tag{5}$$

Since $\mu_B B \ll \Delta_{ex}$, Taylor expansion yields

$$j = A^* T^2 \exp\left(-\frac{e\Phi_B}{k_B T}\right)\cosh\left(\frac{\Delta_{ex}}{2k_B T}\right)\left[1 + P\frac{\mu_B B}{k_B T} + \left(\frac{\mu_B B}{k_B T}\right)^2\right] \times\left[\exp\left(\frac{eU}{nk_B T}\right) - 1\right], \quad (6)$$

with the spin polarization in zero field $P=\tanh(\Delta_{ex}/2k_BT)$. Equation (7) is only valid for the simplified semiconductor band structure depicted in the inset to Fig. 4(b). The current $I=jS$ in a magnetic field is obtained as

$$I(B) = I(0)\left[1 + P\frac{\mu_B B}{k_B T} + \left(\frac{\mu_B B}{k_B T}\right)^2\right], \quad (7)$$

$$I(0) = SA^* T^2 \exp\left(-\frac{e\Phi_B}{k_B T}\right)\cosh\left(\frac{\Delta_{ex}}{2k_B T}\right)\left[\exp\left(\frac{eU}{nk_B T}\right) - 1\right]. \quad (8)$$

At constant current and in the limit $P\mu_B B/(k_B T) \ll 1$ the voltage is given by

$$U \simeq \frac{nk_B T}{e}\left[\ln\left(1 + \frac{I}{I_{S\Delta}}\right) - \frac{I}{I + I_{S\Delta}} P\frac{\mu_B B}{k_B T}\right], \quad (9)$$

with $I_{S\Delta}=I_S\cosh(\Delta_{ex}/(2k_BT))$. In this limit the magnetoresistance will be linear in the magnetic field. If the magnetic field is antiparallel to the spin polarization, the sign of the B-dependent term changes and a positive magnetoresistance is expected in this model. According to Eq. (8) the ratio of the current measured in zero field and in a finite field, $I(B)/I(0)$, should only be a function of the field and not of the applied voltage. Figure 4(a) shows this ratio as determined experimentally at 120 K for various magnetic fields. Indeed, there is a finite voltage range where a constant ratio is observed. The deviations at large positive and negative voltages might be due to deviations from thermionic emission theory. The values of the ratio $I(B)/I(0)$ were determined in the plateau regime for further analysis. These values depend linearly on the applied field for fields larger than 2 T; at smaller fields domain reversal processes yield a nonlinear field dependence, since the directions of applied magnetic fields and spin polarization vectors must not be parallel any more. Since the slope of the linear dependence is directly proportional to the spin polarization, P was derived from these and similar data obtained at various temperatures and is shown in Fig. 4(b). Alternatively, P can be derived from the magnetoresistance [see Eq. (9)], and the magnetoresistance data as presented in Fig. 3. The corresponding values are shown in Fig. 4(b); these agree well with the data from the analysis of the current-voltage curves. Direct fitting of the magnetoresistance curves is difficult, since this would involve detailed knowledge of the domain structure.

The spin polarization has a value of about 0.6 with a trend to a maximum near the Verwey temperature and a slight decrease at higher temperature. This value is in agreement with an experimental value derived from iron oxide tunneling junctions[17] as well as with theoretical investigations on the optical and tunneling spin polarization.[14,15] The sign of the spin polarization is positive opposite to the spectroscopic spin polarization; this is reminiscent of the situation for Ni and Co.[19] Using $P=\tanh(\Delta_{ex}/2k_BT)$ the temperature dependence of the exchange splitting could be derived from the spin polarization. However, this yields only an effective value that is valid for the simplified band structure shown in the inset to Fig. 4(b), but has no direct meaning for the real band structure of magnetite. Our analysis hinges on the assumption that Eq. (7) is still valid in the case of more complicated band structures, provided that the spin polarization P is treated as an effective parameter. In future work a more realistic band structure should be incorporated into the model.

This work was supported by the DFG under Contract No. DFG ES 86/7-3 within the Forschergruppe "Oxidische Grenz-flächen."

*Electronic address: ziese@physik.uni-leipzig.de

†Present address: Max-Planck-Institut für Chemische Physik fester Stoffe, Nöthnitzer Strasse 40, D-01187 Dresden, Germany

[1] J. M. D. Coey *et al.*, Adv. Phys. **48**, 167 (1999).
[2] M. Ziese, Rep. Prog. Phys. **65**, 143 (2002).
[3] A. Fert and H. Jaffrès, Phys. Rev. B **64**, 184420 (2001).
[4] J. D. Albrecht and D. L. Smith, Phys. Rev. B **66**, 113303 (2002).
[5] D. Korošak and B. Cvikl, Solid State Commun. **130**, 765 (2004).
[6] C. Mitra *et al.*, Appl. Phys. Lett. **79**, 2408 (2001).
[7] H. Tanaka *et al.*, Phys. Rev. Lett. **88**, 027204 (2002).
[8] J. R. Sun *et al.*, Europhys. Lett. **66**, 868 (2004).
[9] A. Yanase and N. Hamada, J. Phys. Soc. Jpn. **68**, 1607 (1999).
[10] Y. S. Dedkov *et al.*, Phys. Rev. B **65**, 064417 (2002).
[11] E. J. W. Verwey, Nature (London) **144**, 327 (1939).
[12] F. Walz, J. Phys.: Condens. Matter **14**, R285 (2002).
[13] D. Ihle and B. Lorenz, J. Phys. C **19**, 5239 (1986).
[14] S. F. Alvarado and P. S. Bagus, Phys. Lett. **67A**, 397 (1978).
[15] C. Srinitiwarawong and G. Gehring, J. Phys.: Condens. Matter **13**, 7987 (2001).
[16] I. I. Mazin, Phys. Rev. Lett. **83**, 1427 (1999).
[17] P. Seneor *et al.*, Appl. Phys. Lett. **74**, 4017 (1999).
[18] S. M. Sze, *Physics of Semiconductor Devices* (Wiley Interscience, New York, 1969).
[19] R. Meservey and P. M. Tedrow, Phys. Rep. **238**, 173 (1994).